

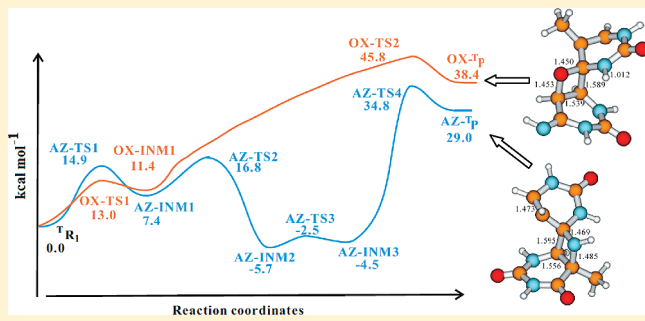
A Theoretical Rationale for Why Azetidine Has a Faster Rate of Formation Than Oxetane in TC(6–4) Photoproducts

Zhao bo Yang,[†] Leif A. Eriksson,[‡] and Ru bo Zhang^{*,†}

[†]Institute for Chemical Physics, Key Laboratory of Cluster Science, Beijing Institute of Technology, Beijing 100081, China

[‡]School of Chemistry, National University of Ireland, Galway, Ireland

ABSTRACT: The mechanism of formation of azetidine and oxetane in (6–4) photoproducts between thymine and imine-type cytosine is studied using the MPWB1K and B3LYP functionals together with the 6-31G(d,p) and 6-311++G(d,p) basis sets, in vacuum and bulk solvent. The photoinduced cycloaddition displays favorable energy barriers in the triplet excited state for formation of both azetidine and oxetane. The stepwise cycloaddition in the triplet excited state involves the initial formation of a diradical followed by ring closure via singlet–triplet interaction. The distinguishing feature in the formation of azetidine compared to that of oxetane is an intermediate H3' back-transfer to N3', which is a low-barrier exothermic reaction, and thus shifts the energy balance toward azetidine formation.



intermediate has been recorded in far-UV-induced 5'C-T3' stacking pairs.^{11,12}

UV absorption of nucleic acids initially produces localized singlet excited states with high photostability. Ultrafast internal conversion channels have been identified by measuring fluorescence lifetimes^{13–15} and through computational studies,^{16–22} revealing the behavior of DNA self-protection from photoinduced lesions. Along the internal conversion of singlet excited states, low-lying triplet excited states can become populated by an intersystem crossing (ISC) mechanism. In addition, some triplet excited state photosensitizers possess sufficiently high energy to photosensitize thymine bases, whose triplet energy is the lowest among those of the natural nucleobases.²³ The transition of thymine to the T₁ state, located 3.6 eV above the ground state, was also identified in earlier theoretical studies.^{24,25}

Our previous calculations have shown that the formation of CPD displays favorable energy barriers and reaction energies in both the triplet and singlet excited states.²⁶ The stepwise cycloaddition in the triplet excited state involves the initial formation of a diradical, followed by ring closure via singlet–triplet interaction. In the case of the TT64 photoproduct, formation of the oxetane intermediate not only depends on the conformation of the two bases but also requires population of the reactive state.^{27,28} The aim of this study is to elucidate by theoretical means the mechanism of azetidine and oxetane formation from the T-IC pair on the lowest-lying triplet excited state surface, and the possible interaction between the lowest-lying triplet and singlet states. The study sheds light on why the formation of

1. INTRODUCTION

Ultraviolet (UV) irradiation of cells causes the formation of a variety of DNA lesions, many of which are known to have mutagenic, carcinogenic, and lethal effects.^{1,2} The main UV lesions are cyclobutane-pyrimidine dimers (CPD lesions) formed in a photochemically allowed [2+2] cycloaddition and (6–4) photoproducts (64PP). The latter are presumably more mutagenic.³ The highly mutagenic (6–4) lesions are believed to be formed between two adjacent pyrimidines in the DNA duplex to initially give a four-membered ring intermediate. Both types of DNA lesions are repaired by DNA photolyases, which cleave the lesions back into the monomers in a light-dependent single-electron transfer repair reaction.⁴

64PP has been detected mainly in thymine-thymine (TT) and thymine-cytosine (TC) stacking pairs.⁵ Experiments have showed that the rates of formation of (6–4) photoproducts in different sequences are in the following order: 5'T-C3' \gg 5'T-T3' > 5'C-T3'.^{6,7} This shows that the relative orientation and structural features of both thymine and cytosine may be factors controlling the rate of formation of (6–4) photoproducts. TT64 is proven to be an OH transfer species formed via a short-lived oxetane ring intermediate. It is thus reasonable to assume that the formation of TC64, which is characterized by an amino group transfer to the 5 position of the 5' thymine, is analogous to the pathway for formation of the TT64 product, namely, through an azetidine ring intermediate. The imine-type tautomer of cytosine (IC) is thought to participate in the formation of the azetidine.⁸ It is, however, well-known that keto-type cytosine is more stable than the imine form in the singlet ground state.⁹ The possible existence of IC has been attributed to proton transfer reactions between the hydrogen bonding guanine-cytosine base pair in the triplet excited state.¹⁰ In addition, the oxetane

Received: May 14, 2011

Revised: June 15, 2011

Published: June 19, 2011

azetidine is favored over that of oxetane, with the hope that this work will contribute to further studies of the mechanism of TC64 formation.

2. COMPUTATIONAL METHODS

The standard B-type dinucleotide 5'-T-C3' was selected for the subsequent optimizations and reactions. Two-layer ONIOM calculations were used to optimize the dinucleotide in both the singlet ground state and the triplet excited state. The keto-type

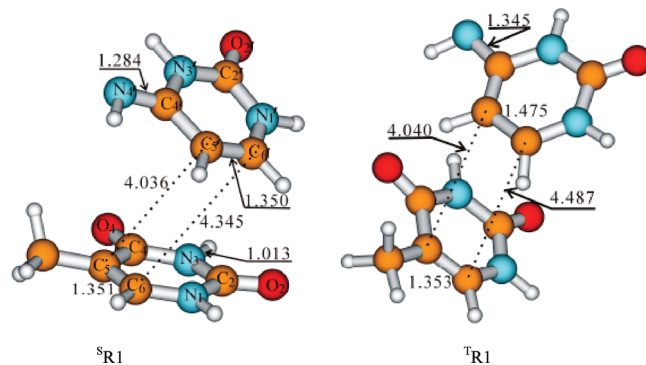


Figure 1. Optimized structures of initial reactants in singlet and lowest excited triplet states [MPWB1K/6-31+G(d,p):Amber03 level].

Table 1. Mulliken Spin Densities [e^- ; B3LYP/6-311++G(d,p) level] of Selected Atoms in Each Species along the Triplet Thymine-Cytosine Cycloaddition Reactions^a

	C4'	N4'	CS'	C6'	C5	C6	C4	O4
T _{R1}	0.14	0.68	0.63	0.73	—	—	—	—
AZ-TS1	—	0.31	—	—	—	0.8	—	—
AZ-INM1	—	—	—	—	-0.18	0.86	0.87	0.12
AZ-TS2	—	—	—	—	-0.12	0.84	0.66	0.16
AZ-INM2	0.47	—	0.54	—	-0.12	0.92	—	—
AZ-TS3	0.47	—	-0.17	0.53	—	0.87	—	—
AZ-INM3	0.51	—	-0.21	0.52	-0.10	0.93	—	—
AZ-TS4	-0.20	—	0.8	0.79	—	0.32	—	—
AZ-T ^P	—	—	0.98	0.84	—	-0.19	—	—
OX-TS1	—	0.15	0.16	0.72	—	0.43	0.26	0.12
OX-INM1	—	—	—	0.86	—	0.55	0.35	—
OX-TS2	—	—	—	0.43	0.93	0.73	-0.4	—
OX-T ^P	—	—	—	—	0.95	0.87	—	—

^aComponents smaller than 0.1 are neglected in the table.

Table 2. Relative Energies (kilocalories per mole) of the Species along the Triplet Thymine-Cytosine Addition Reaction^a

reaction	6-31G(d,p)		6-311++G(d,p)			
	TS ^b	RE ^b	TS ^b	RE ^b	TS ^c	RE ^c
T _{R1} → AZ-TS1 → AZ-INM1	13.7	6.0	14.9 (15.4) ^d	7.4 (7.3) ^d	14.1	9.3
AZ-INM1 → AZ-TS2 → AZ-INM2	9.0	-13.1	9.4 (7.2) ^d	-13.1 (-11.8) ^d	5.7	-13.4
AZ-INM2 → AZ-TS3 → AZ-INM3	1.7	1.7	3.2	1.2	3.3 (2.9) ^d	1.3 (1.4) ^d
AZ-INM3 → AZ-TS4 → AZ-T ^P	39.2	32.3	39.3 (38.8) ^d	33.5 (33.0) ^d	38.4	33.6
T _{R1} → OX-TS1 → OX-INM1	12.1	8.4	13 (13.4) ^d	11.4 (13.0) ^d	13.5	12.8
OX-INM1 → OX-TS2 → OX-T ^P	34.8	26.7	34.4 (33.7) ^d	27.0 (26.6) ^d	34.1	27.9

^aAbbreviations: RE, reaction energy; TS, reaction barrie. ^bWith ZPE corrections. ^cWithout ZPE corrections. ^dValues in parentheses include PCM corrections.

thymine (T) and imine-type cytosine (IC) bases were treated at a high level using the MPWB1K/6-31+G(d,p) method,²⁹ and the sugar and phosphate groups were treated using the Amber force field.³⁰ Frequency calculations were performed to characterize the stationary points. The MPWB1K functional has previously been shown to perform well for weakly interacting systems,³¹ but it is relatively untested for excited state systems. Consistent with our previous studies,^{26,28} the optimized structures were modified through the replacement of sugar and phosphate groups with two H atoms. The obtained base pair was further optimized using the B3LYP/6-31G(d,p) method,³² restraining the key intermolecular distances [$R(C5-C5') = 4.040 \text{ \AA}$, and $R(C6-C6') = 4.487 \text{ \AA}$] as obtained from the ONIOM[MPWB1K/6-31+G(d,p):Amber03] calculations described above, displayed in Figure 1. The computational model system focuses on the formation of the biologically relevant TC64 lesion, and B3LYP was employed for the main body of the study because of its vast use in excited state calculations and to allow comparison with earlier studies on related systems. Neglect of the influence of the DNA backbone (e.g., strain effects) and the complementary strand (e.g., hydrogen bond interactions) on the reacting bases is necessitated by the need to calculate numerous structures through which the systems pass en route between reactants and products, as outlined below. Even though the surrounding DNA and the presence of a solvent most certainly affect the photodimerization, it may be noted that the absorption of light by DNA results in localization of energy primarily at the sites of the conjugated nucleobases.

Each structure on the potential energy surface (PES) was optimized using the B3LYP hybrid density functional in conjunction with the 6-31G(d,p) basis set. B3LYP/6-31G(d,p) frequency calculations were performed to identify the stationary points as either minima (reactant complexes and product structures) or first-order saddle points (transition structures) and to extract zero-point vibrational energy (ZPE) corrections. Bulk solvation effects were included using the integral electron formalism of the polarized continuum model (IEF-PCM).³³ B3LYP/6-311++G(d,p) calculations were performed for the final single-point energy calculations in conjunction with the PCM approach. All calculations were performed using the Gaussian 03 suite of programs.³⁴

3. RESULTS AND DISCUSSION

3.1. Structures of the T-IC Dinucleotide Complex. The optimized structures of the T-IC pair are shown in Figure 1. For the singlet T-IC complex, the MPWB1K/6-31+G(d,p):

Amber03 optimization gives C5–C5' and C6–C6' distances of 4.036 and 4.345 Å, respectively. In the standard B-type DNA, they are 4.036 and 4.470 Å, respectively. Both the C5–C6 and C5'–C6' bond lengths are ~1.350 Å, characteristic of a C=C double bond. For the optimized triplet T-IC pair, the C5–C5' and C6–C6' distances are 4.040 and 4.487 Å, respectively. The C5–C6 bond length of the thymine fragment remains almost intact, while the C5'–C6' bond length of IC is extended to 1.475 Å. It is thus essentially a σ bond, and the two unpaired electrons mainly populate the C5' (0.63 e⁻) and C6' (0.73 e⁻) atoms (Table 1). In addition, the C4'–N4' bond of IC is elongated to 1.345 Å, which is longer than that for IC in the corresponding singlet complex, showing that the unpaired electrons also populate these sites. The adiabatic singlet–triplet gap is estimated to be ~2.80 eV at both the B3LYP/6-31G(d,p) and B3LYP/6-311++G(d,p) levels without ZPE corrections and 2.67 eV when ZPE effects are included. These values are considerably lower than the singlet–triplet gap of keto-type thymine,^{25,26} but close to those of imine-type cytosine.³⁵

3.2. Formation of the Azetidine Intermediate. The energy profiles of the triplet cycloaddition reactions are listed in Table 2. The pathway for the formation of the azetidine intermediate on the triplet PES proceeds through an initial attack by N4' on C5, with a concerted transfer of H3' to the neighboring O4 of thymine. The corresponding geometries are displayed in Figure 2. From ^TR1 to AZ-INM1, the activation energy is 13.7 kcal/mol at the B3LYP/6-31G(d,p) level and 14.9 kcal/mol at the B3LYP/6-311++G(d,p) level, without ZPE corrections. The reaction energy relative to ^TR1 is estimated to be 6.0 kcal/mol at the B3LYP/6-31G(d,p) level and 7.4 kcal/mol at the B3LYP/6-311++G(d,p) level, without ZPE corrections. In the AZ-TS1 transition structure, the N4'···C5 distance is 2.053 Å and the C5–C6 bond length is extended to 1.423 Å. The increase in the C4–O4 bond length is a result of the proton transferred from N3' to O4. The resulting intermediate AZ-INM1 is a diradical with spin densities localized to C4 (0.87) and C6 (0.86).

For AZ-INM1, the H2'···N3' hydrogen bond length is 1.715 Å. Under the assumption that H3' will back-transfer to N3', the reaction barrier is calculated to be 9.4 kcal/mol without and 5.7 kcal/mol with ZPE corrections at the B3LYP/6-311++G(d,p) level. The reaction energy from AZ-INM1 to AZ-INM2 is exothermic by 13.4 kcal/mol (including ZPE corrections) at the same level. The N4'–C5 bond length is contracted from 1.527 Å in AZ-INM1 to 1.477 Å in AZ-INM2, which also accounts for the higher stability of AZ-INM2 versus AZ-INM1. Thus, the return of H3' to N3' appears to be essential for the formation of a stable azetidine intermediate.

Through a rotation around the N4'–C5 bond, AZ-INM2 proceeds to AZ-TS3 and AZ-INM3, with a relative barrier of 3.3 kcal/mol at the B3LYP/6-311++G(d,p) level (including ZPE corrections). The energy difference between AZ-INM2 and AZ-INM3 is 1.3 kcal/mol, in favor of the former. The formation of azetidine from AZ-INM3 is finally accomplished through C4' cross-linking to C6. The ring closure barrier on the triplet surface from AZ-INM3 to AZ-TS4 is as expected quite high, 38.4 kcal/mol. The relative reaction energy furthermore has a considerable endothermic character: 32.5 and 33.6 kcal/mol (without and with ZPE corrections, respectively), at the B3LYP/6-311++G(d,p) level. The structure of the obtained triplet azetidine is characterized by a puckered pyrimidone, whereas in the singlet counterpart, both pyrimidine and pyrimidone rings are planar.

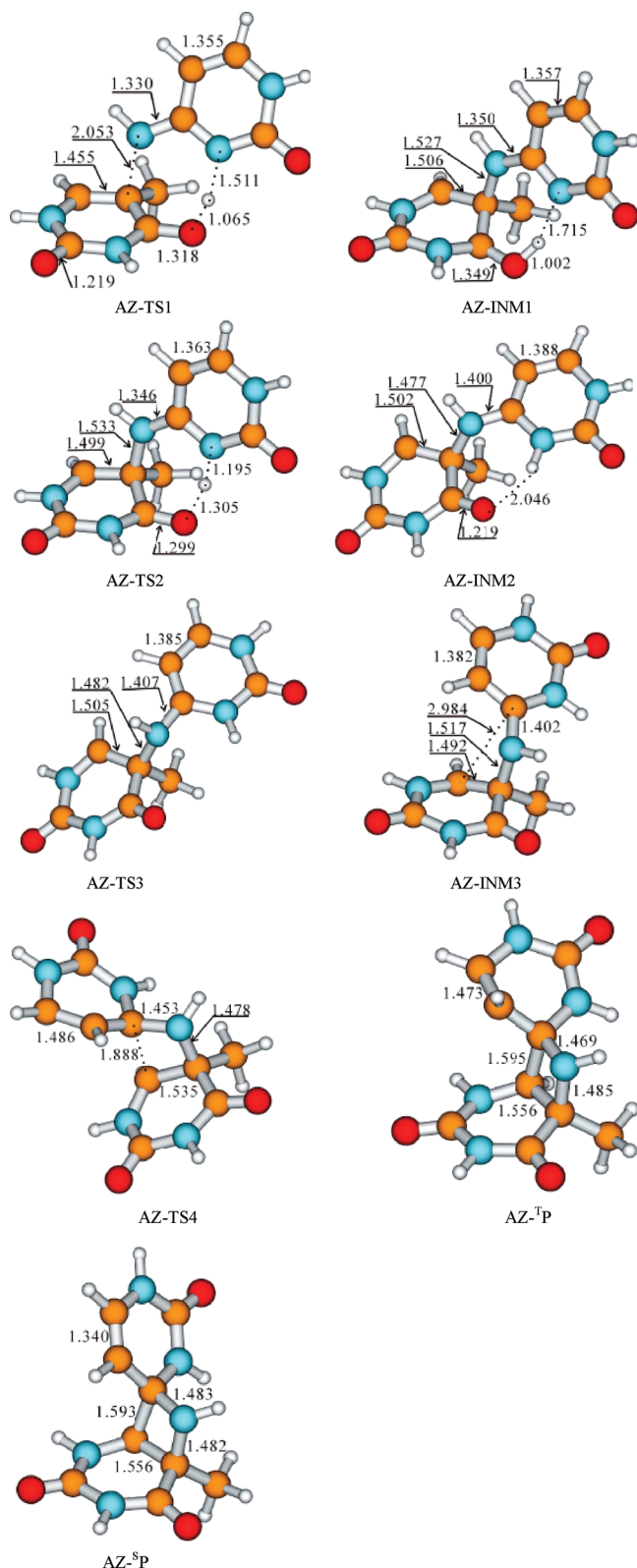


Figure 2. Optimized stationary structures along pathways for azetidine formation [B3LYP/6-31G(d,p) level].

In Figure 3, we display the energy surfaces for the triplet state reaction. According to the results described above, the azetidine intermediate will not be formed on the triplet PES alone, because

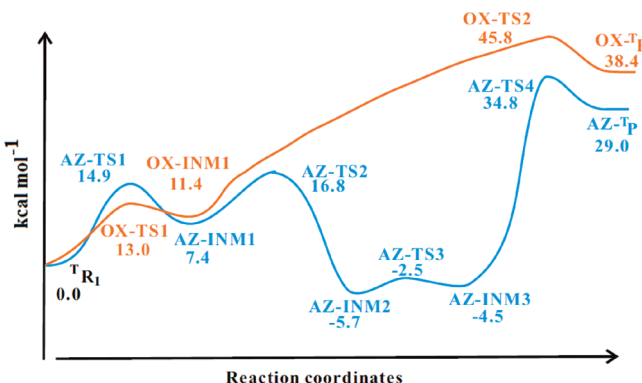


Figure 3. Triplet energy surfaces for azetidine (blue) and oxetane (orange) formation.

of the high barrier for the $\text{AZ-INM3} \rightarrow \text{AZ-TS4} \rightarrow \text{AZ-}^{\text{T}}\text{P}$ reaction. These results as such do not agree in full with the results implied by various experiments. To this end, the interaction between the lowest-lying triplet and the singlet ground state surface is important for an improved understanding of triplet azetidine formation.

To obtain a reliable singlet–triplet interaction profile, we scanned the PES from AZ-INM3 to AZ-^TP by varying the C4'…C6 distances with a step length of 0.1 Å, constraining the N4'…C5 distance to 1.517 Å, and optimizing the remaining coordinates. The energies for the singlet–triplet scans are displayed in Figure 4A (starting from AZ-INM3, far right). As seen, there is a crossing point between the singlet and triplet surfaces at the C4'…C6 distance of 2.339 Å with an energy of ca. −849.21333 au at the B3LYP/6-311++G(d,p) level. The energy gap between the crossing point and AZ-INM3 is approximately 10.8 kcal/mol. The mechanism is essentially identical when bulk solvent is included. The determined energy barriers to the spin crossover are dramatically lower than the 32.5 kcal/mol barrier for the triplet ring closure reaction, indicating that singlet–triplet state interaction is a possible channel to the formation of azetidine.

3.3. Formation of the Oxetane Intermediate. The alternative competing pathway leading to the formation of oxetane on the triplet PES proceeds via an initial cross-linking between O4 of thymine and C6' of triplet IC, followed by subsequent formation of the C4–C6' bond. The geometries along the reaction path are shown in Figure 5.

The first step in the cross-link reaction occurs between the O4 and C6' atoms in ^TR1. From ^TR1 to OX-INM1, the activation energy is 12.1 kcal/mol at the B3LYP/6-31G(d,p) level and 13.0 kcal/mol at the B3LYP/6-311++G(d,p) level, without ZPE corrections. The reaction energy is estimated to be 8.4 kcal/mol at the B3LYP/6-31G(d,p) level and 11.4 kcal/mol at the B3LYP/6-311++G(d,p) level. These values are comparable to those for the reaction from ^TR1 to AZ-INM1. The distance from O4 to C6' is 1.847 Å in OX-TS1 and 1.482 Å in OX-INM1. The second step in the cross-link formation, between C4' and C5 atoms of OX-INM1, leads to the ring-closed product OX-^TP (oxetane structure). The reaction barrier is 34.1 kcal/mol at the B3LYP/6-311++G(d,p) level. The relative reaction energy is endothermic, as for the formation of azetidine, by 27.9 kcal/mol. As in the azetidine case, the formation of oxetane on the triplet only surface is highly unlikely (cf. Figure 3).

As in the azetidine reaction, a singlet–triplet interaction profile was obtained by scanning the PES from OX-INM1 to

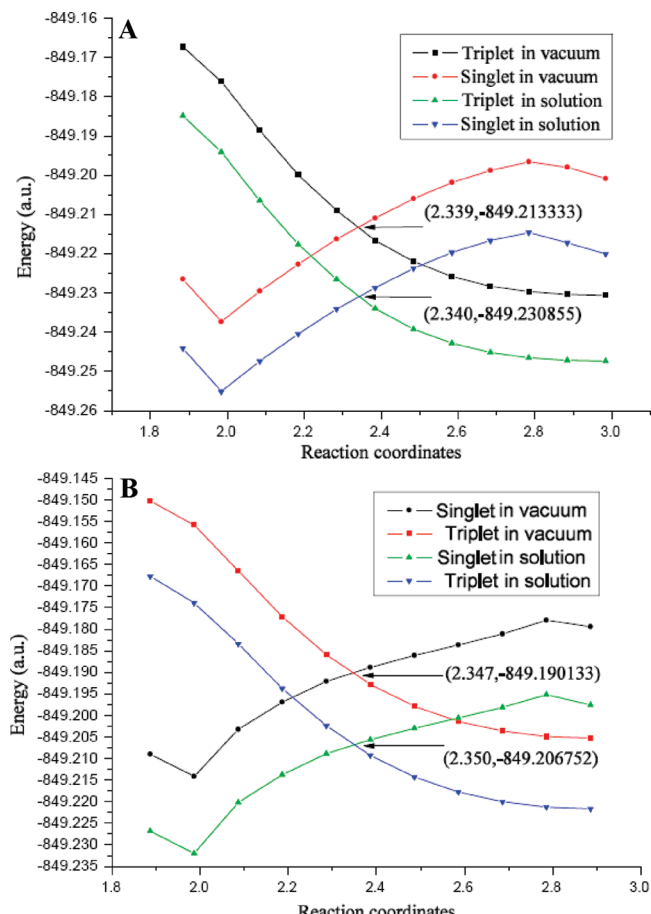


Figure 4. Scanned singlet and triplet energy surfaces from (A) AZ-INM3 (far right) to AZ-TS4/AZ-^TP (left side) and (B) OX-INM1 (far right) to OX-TS2/OX-^TP (left side).

OX-^TP by varying the C4…C6' distances with a step length of 0.1 Å, constraining the O4…C5' distance to 1.482 Å, and optimizing the remaining coordinates. The energies for the singlet–triplet scans are displayed in Figure 4B (starting from OX-INM1 at the far right). Along the OX-INM1 to OX-^TP pathway, a crossing point is observed at a C4…C6' distance of 2.347 Å with an energy of ca. −849.19013 au at the B3LYP/6-311++G(d,p) level. The estimated energy gap between the crossing point and OX-INM1 is thus approximately 9.5 kcal/mol. The determined energy barrier to the spin crossover is hence also in this case dramatically lower than the 34.1 kcal/mol barrier required for the triplet ring closure reaction, indicating that singlet–triplet state interaction is a possible channel also in the formation of the oxetane. The structure of the obtained triplet oxetane is characterized by a puckered pyrimidone, whereas in the singlet counterpart, both the pyrimidine and pyrimidone remain planar.

The influence of bulk solvation with an ϵ of 4.0 was also calculated, and the relative values are presented in Table 2 and Figure 4A,B. The values show that the reaction energy profiles are unchanged by the bulk solvent.

Via comparison of the two reactions, the barriers from the initial ^TR1 to both AZ-INM1 and OX-INM1 are comparable, as are the reaction energies. In addition, the determined energy barriers from AZ-INM3 and OX-INM1 to the corresponding spin crossover points are almost identical (within ~1 kcal/mol).

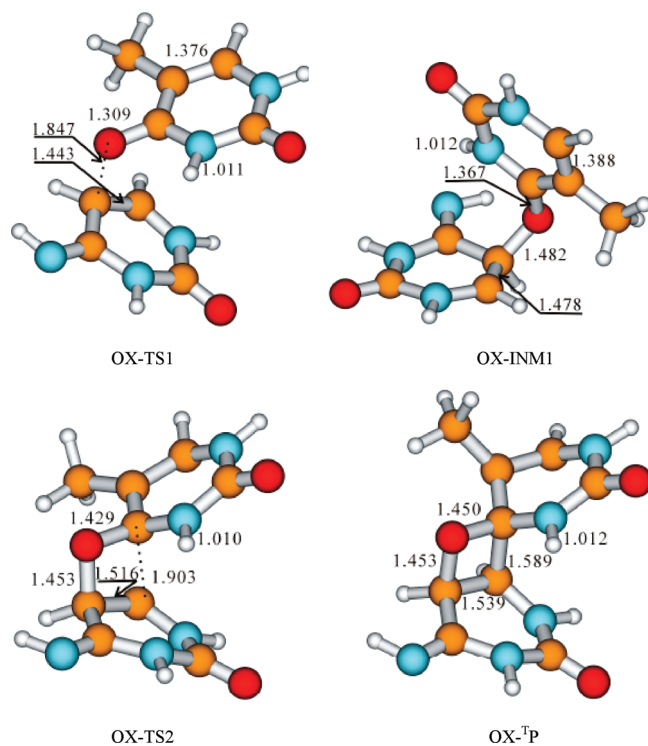


Figure 5. Optimized stationary structures along pathways for oxetane formation [B3LYP/6-31G(d,p) level].

The distinction between the formation of azetidine and oxetane is that H3' needs to be back-transferred to N3' for the formation of azetidine. This is a low-barrier exothermic reaction, which promotes the formation of azetidine, and can possibly be one of the reasons why the rate of formation of azetidine is greater than that of oxetane.

4. CONCLUSIONS

In this work, the processes of both azetidine and oxetane formation in the T-IC base pair in the lowest-lying triplet excited states are explored with an objective of determining their reaction energy profiles. Geometries were obtained at the B3LYP/6-31G(d,p) level of theory in the gas phase, followed by energy calculations at the B3LYP/6-311++G(d,p) level in the gas phase and in solution ($\epsilon = 4.3$) using the IEF-PCM model. Stepwise pathways to formation of both azetidine and oxetane are found on the triplet PES. For the initial reactions on the triplet PES in the gas phase, the barriers range from 13.5 to 14.1 kcal/mol and the reaction energies are slightly endothermic, resulting in the formation of diradical intermediates. After formation of the initial single cross-linked products, proton back-transfer to the IC fragment is a significant, exothermic process, which favors the formation of azetidine over oxetane. The final ring closing reactions are for both systems prohibited by high energy barriers. Instead, the interaction between triplet and singlet states plays a significant role in the formation of both products and provides >20 kcal/mol lower barriers to ring closure. These data provide a rationale for the observation that triplet mechanisms may be involved in the formation of azetidine and oxetane in the T-IC base pair. Proton back-transfer is found to be a key step, which promotes a faster formation of azetidine over oxetane in accord with experimental data.

AUTHOR INFORMATION

Corresponding Author

*E-mail: zhangrubo@bit.edu.cn.

ACKNOWLEDGMENT

The National University of Ireland is gratefully acknowledged for financial support. This work is also supported by the National Nature Science Foundation of China (Grants 20643007 and 20703004).

REFERENCES

- (1) de Gruij, F. R. *Methods Enzymol.* **2000**, *319*, 359–366.
- (2) Matsumura, Y.; Ananthaswamy, H. N. *Toxicol. Appl. Pharmacol.* **2004**, *195*, 298–308.
- (3) Glickman, B. W.; Schaaper, R. M.; Haseltine, W. A.; Dunn, R. L.; Brash, D. E. *Proc. Natl. Acad. Sci. U.S.A.* **1986**, *83*, 6945–6949.
- (4) Glas, A. F.; Schneider, S.; Maul, M. J.; Hennecke, U.; Carell, T. *Chem.—Eur. J.* **2009**, *15*, 10387–10396.
- (5) Cadet, J.; Sage, E.; Douki, T. *Mutat. Res.* **2005**, *571*, 3–17.
- (6) Matallana-Surgeta, S.; Meador, J. A.; Joux, F.; Douki, T. *Photochem. Photobiol. Sci.* **2008**, *7*, 794–801.
- (7) Courdavault, S.; Baudouin, C.; Charveron, M.; Canguilhem, B.; Favier, A.; Cadet, J.; Douki, T. *DNA Repair* **2005**, *4*, 836–844.
- (8) (a) CHnguen, P. H.; Arieti, C. F.; Roza, L.; Mori, T.; Nikaido, O.; Green, M. H. L. *Cancer Res.* **1995**, *55*, 2245–2248. (b) Douki, T.; Voituriez, L.; Cadet, J. *Chem. Res. Toxicol.* **1995**, *8*, 244–253.
- (9) Kobayashi, R. *J. Phys. Chem. A* **1998**, *102*, 10813–10817.
- (10) (a) Lamola, A. A.; Gueron, M.; Yamane, T.; Eisinger, J.; Shulman, R. G. *J. Chem. Phys.* **1967**, *47*, 2210–2217. (b) Blancafort, L.; Bertran, J.; Sodupe, M. *J. Am. Chem. Soc.* **2004**, *126*, 12770–12771.
- (11) Douki, T.; Cadet, J. *J. Photochem. Photobiol. B* **1992**, *15*, 199–213.
- (12) Douki, T.; Voituriez, L.; Cadet, J. *Chem. Res. Toxicol.* **1995**, *8*, 244–253.
- (13) Crespo-Hernandez, C. E.; Cohen, B.; Hare, P. M.; Kohler, B. *Chem. Rev.* **2004**, *104*, 1977–2019.
- (14) Pecourt, J.-M. L.; Peon, J.; Kohler, B. *J. Am. Chem. Soc.* **2000**, *122*, 9348–9349.
- (15) Pecourt, J.-M. L.; Kohler, B.; Peon, J. *J. Am. Chem. Soc.* **2001**, *123*, 5166–5166.
- (16) Sobolewski, A. L.; Domcke, W. *Eur. Phys. J. D* **2002**, *20*, 369–374.
- (17) Ismail, N.; Blancafort, L.; Olivucci, M.; Kohler, B.; Robb, M. A. *J. Am. Chem. Soc.* **2002**, *124*, 6818–6819.
- (18) Merchan, M.; Serrano-Andres, L. *J. Am. Chem. Soc.* **2003**, *125*, 8108–8109.
- (19) Blancafort, L.; Robb, M. A. *J. Phys. Chem. A* **2004**, *108*, 10609–10614.
- (20) Zgierski, M. Z.; Patchkovskii, S.; Fujiwara, T.; Lim, E. C. *J. Phys. Chem. A* **2005**, *109*, 9384–9387.
- (21) Merchan, M.; Serrano-Andres, L.; Robb, M. A.; Blancafort, L. *J. Am. Chem. Soc.* **2005**, *127*, 1820–1825.
- (22) González-Vázquez, J.; González, L.; Samoylovab, E.; Schultz, T. *Phys. Chem. Chem. Phys.* **2009**, *11*, 3927–3934.
- (23) (a) Encinas, S.; Belmadoui, N.; Climent, M. J.; Gil, S.; Miranda, M. A. *Chem. Res. Toxicol.* **2004**, *17*, 857–862. (b) Chouini-Lalanne, N.; Defais, M.; Paillous, N. *Biochem. Pharmacol.* **1998**, *55*, 441–446.
- (24) Abouaf, R.; Pommier, J.; Dunet, H. *Chem. Phys. Lett.* **2003**, *381*, 486–494.
- (25) Nguyen, M. T.; Zhang, R.; Nam, P.-C.; Ceulemans, A. *J. Phys. Chem. A* **2004**, *108*, 6554–6561.
- (26) Zhang, R. B.; Eriksson, L. A. *J. Phys. Chem. B* **2006**, *110*, 7556–7562.
- (27) McCullagh, M.; Hariharan, M.; Lewis, F. D.; Markovitsi, D.; Douki, T.; Schatz, G. C. *J. Phys. Chem. B* **2010**, *114*, 5215–5221.

(28) Yang, Z. B.; Zhang, R. B.; Eriksson, L. A. *Phys. Chem. Chem. Phys.* **2011**, *13*, 8961–8966.

(29) (a) Zhao, Y.; Truhlar, D. G. *J. Phys. Chem. A* **2004**, *108*, 6908–6918. (b) Zhao, Y.; Truhlar, D. G. *J. Chem. Theory Comput.* **2005**, *1*, 415–432.

(30) Cornell, W. D.; Cieplak, P.; Bayly, C. I.; Gould, I. R.; Merz, K. M.; Ferguson, D. M.; Spellmeyer, D. C.; Fox, T.; Caldwell, J. W.; Kollman, P. A. *J. Am. Chem. Soc.* **1995**, *117*, 5179–5197.

(31) Dkhissi, A.; Blossey, R. *Chem. Phys. Lett.* **2007**, *439*, 35–39.

(32) (a) Lee, C.; Yang, W.; Parr, R. G. *Phys. Rev. B* **1988**, *37*, 785–789. (b) Becke, A. D. *J. Chem. Phys.* **1993**, *98*, 5648–5652.

(33) Mennucci, B.; Tomasi, J. *J. Chem. Phys.* **1997**, *106*, 5151–5158.

(34) Frisch, M. J.; Trucks, G. W.; Schlegel, H. B.; Scuseria, G. E.; Robb, M. A.; Cheeseman, J. R.; Montgomery, J. A., Jr.; Vreven, T.; Kudin, K. N.; Burant, J. C.; Millam, J. M.; Iyengar, S. S.; Tomasi, J.; Barone, V.; Mennucci, B.; Cossi, M.; Scalmani, G.; Rega, N.; Petersson, G. A.; Nakatsuji, H.; Hada, M.; Ehara, M.; Toyota, K.; Fukuda, R.; Hasegawa, J.; Ishida, M.; Nakajima, T.; Honda, Y.; Kitao, O.; Nakai, H.; Klene, M.; Li, X.; Knox, J. E.; Hratchian, H. P.; Cross, J. B.; Adamo, C.; Jaramillo, J.; Gomperts, R.; Stratmann, R. E.; Yazyev, O.; Austin, A. J.; Cammi, R.; Pomelli, C.; Ochterski, J. W.; Ayala, P. Y.; Morokuma, K.; Voth, G. A.; Salvador, P.; Dannenberg, J. J.; Zakrzewski, V. G.; Dapprich, S.; Daniels, A. D.; Strain, M. C.; Farkas, O.; Malick, D. K.; Rabuck, A. D.; Raghavachari, K.; Foresman, J. B.; Ortiz, J. V.; Cui, Q.; Baboul, A. G.; Clifford, S.; Cioslowski, J.; Stefanov, B. B.; Liu, G.; Liashenko, A.; Piskorz, P.; Komaromi, I.; Martin, R. L.; Fox, D. J.; Keith, T.; Al-Laham, M. A.; Peng, C. Y.; Nanayakkara, A.; Challacombe, M.; Gill, P. M. W.; Johnson, B.; Chen, W.; Wong, M. W.; Gonzalez, C.; Pople, J. A. *Gaussian 03*; Gaussian, Inc.: Wallingford, CT, 2004.

(35) The singlet–triplet gap of imine-type cytosine is 2.70 eV (with ZPE corrections) or 2.83 eV (without ZPE corrections) at the B3LYP/6-31G(d,p) level or 2.68 eV (with ZPE corrections) or 2.81 eV (without ZPE corrections) at the B3LYP/6-311++G(d,p) level.